

$^{34}\text{S}(p,n)^{34}\text{Cl}$ reaction at 35 MeV and its microscopic distorted-wave Born approximation analysis: Stringent test of the shell model

K. Furukawa, M. Kabasawa, T. Kawamura, Y. Takahashi, A. Satoh, and T. Nakagawa
Department of Physics, Tohoku University, Sendai 980, Japan

H. Orihara, T. Niizeki, and K. Ishii
Cyclotron and Radioisotope Center, Tohoku University, Sendai 980, Japan

K. Maeda
College of General Education, Tohoku University, Sendai 980, Japan

K. Miura
Tohoku Institute of Technology, Sendai 982, Japan

B. A. Brown
Cyclotron Laboratory, Michigan State University, East Lansing, Michigan 48824

H. Ohnuma
Department of Physics, Tokyo Institute of Technology, Oh-okayama, Meguro, Tokyo 152, Japan
(Received 11 August 1987)

Differential cross sections for the $^{34}\text{S}(p,n)^{34}\text{Cl}$ reaction were measured at $E_p = 35$ MeV. Remarkable differences were observed among the angular distribution shapes for the known 1^+ states in ^{34}Cl at 0.441, 0.666, 2.581, and 3.128 MeV. Distorted-wave Born approximation calculations using the recent full sd -shell wave functions of Brown and Wildenthal successfully reproduce such differences, whose origin was traced back to the different contributions of the $\Delta J(\Delta L, \Delta S) = 1(0,1)$ and $1(2,1)$ transition amplitudes. The 1^+ transitions with dominant $1(0,1)$ amplitudes required renormalization factor N of about 0.8, which agrees well with that obtained for the β^+ decay of ^{34}Ar . The 1^+ and 2^+ transitions with dominant $1(2,1)$ and $2(2,1)$ amplitudes required N of about 0.5. Similar distorted-wave Born approximation calculations gave a good description of the $\Delta S = 0$ and $\Delta L = 0$ and 2 transitions without any renormalization.

I. INTRODUCTION

Very recently Brown and Wildenthal¹ (BW) reported a comprehensive comparison of experimentally observed Gamow-Teller (GT) beta decay rates with their theory for the sd -shell nuclei ($A = 17-39$). Their wave functions are based on the complete $(0d_{5/2}, 1s_{1/2}, 0d_{3/2})$ space shell model obtained from diagonalization of a model Hamiltonian which reproduced observed energy-level structure throughout the sd -shell nuclei. These wave functions are currently used extensively. For example, in supernova problems, stellar weak-interaction rates for sd -shell nuclei are calculated² based on the nuclear matrix elements obtained from the sd -shell wave functions in cases where GT transitions have not been measured or in cases where β decays are energetically impossible. Therefore stringent tests of these wave functions are of extreme importance.

Low-energy (p,n) experiments are very attractive in the study of nuclear structure because the high resolution experimentally attainable makes a level-to-level comparison of the (p,n) strength and the β -decay strength possible. The $^{34}\text{S}(p,n)^{34}\text{Cl}$ reaction is especially

interesting since (1) it contains analog transitions which can be used to check optical potential parameters; (2) several $0^+ \rightarrow 1^+$ GT transitions are known from the $^{34}\text{Ar} \rightarrow ^{34}\text{Cl}$ β^+ decay;¹ (3) the renormalization factors $B(\text{GT})_{\text{exp}}/B(\text{GT})_{\text{free}}$ reported by BW for these GT β decays are close to unity, especially for the strong transition to the $^{34}\text{Cl}(3.128 \text{ MeV}, 1^+)$ state, in sharp contrast to an overall reduction factor of about 0.6 in the middle of the sd shell; and (4) a strong transition to a 1^+ state at $E_x = 5$ MeV is predicted by BW, although the β decay of ^{34}Ar to this state is energetically unfavored ($Q_\beta = 6.06$ MeV) and has not been observed.

On the other hand, care must be exercised in the analysis of low-energy (p,n) data because of the strong spin-independent interaction, relative importance of distortion effects and exchange processes, ambiguities in the effective interaction, possible contribution from higher-order processes, etc. In this regard intermediate energy (p,n) reactions are favored albeit with limited energy resolution. Recently we reported³ that low-energy, high resolution (p,n) data provide information basically identical to that obtained at intermediate energies if careful analysis is made. In Ref. 3 the above problems were dis-

cussed in detail for the typical examples of the $^{12}\text{C}(p,n)$ and $^{16}\text{O}(p,n)$ reactions at $E_p = 35$ and 40 MeV.

In this work we report on a high-resolution study of the $^{34}\text{S}(p,n)^{34}\text{Cl}$ reaction at an incident energy of 35 MeV. Detailed comparisons of the results with DWBA calculations with transition amplitudes obtained⁴ from the BW wave functions are made. The results provide a stringent test of these wave functions.

II. EXPERIMENTAL PROCEDURE

The experiment was performed using a 35-MeV proton beam from the AVF cyclotron and the time-of-flight facilities⁵ at the Cyclotron and Radioisotope of Tohoku University. We utilized a beam swinger system, and measured angular distributions of emitted neutrons between 0° and 110° (lab). The target was 2.64 mg/cm^2 in thickness, and enriched to 94.4% in ^{34}S . Sulfur powder was evaporated onto carbon foil of 1 mg/cm^2 thickness, enriched to 99.9% in ^{12}C . Then the sulfur layer was covered by thin gold to avoid evaporation of sulfur during the beam bombardment. Small angle measurements were repeated during the experiment, and no noticeable target deterioration was observed. Overall time resolution was about 1 ns. An absolute calibration of the detector efficiencies was made by measuring emitted neutrons and the ^7Be residual activity in the $^7\text{Li}(p,n)^7\text{Be}$ reaction. Good agreement with a Monte Carlo calculation was found. Errors in the absolute scale of the cross sections were estimated to be $\leq 15\%$ and the relative errors $\leq 7\%$.

III. EXPERIMENTAL RESULTS AND DWBA ANALYSIS

A typical neutron spectrum at a laboratory angle of 20° is shown in Fig. 1 together with a peak fit result. Previously known 1^+ states at 0.461, 0.666, 2.581, and 3.128 MeV, and 2^+ states at 1.23 and 1.89 MeV, are seen to be excited. Also seen in the spectrum are the $T=1$, 0^+ and 2^+ isobaric analog states at 0.0 and 3.38 MeV. A prominent peak is observed at $E_x = 4.985 \pm 0.010$ MeV, where a strong GT transition is predicted by the shell-model calculation as mentioned earlier. However, this peak probably is a doublet as will be discussed later.

In Figs. 2–7 obtained angular distributions of neutrons leading to these states are shown. Curves in these figures are DWBA predictions by the code DWBA-70 (Ref. 6) unless otherwise stated. Optical potential parameters of Becchetti and Greenlees⁷ are used for protons, while those for neutrons are self-consistent potential parameters derived by Carlson *et al.*⁸ The effective nucleon-nucleon interaction of Bertsch *et al.*⁹ (*M3Y*) is used in the DWBA calculations. A Woods-Saxon-type bound-state potential with $r_0 = 1.25 \text{ fm}$, $a = 0.65 \text{ fm}$, and $V_{LS} = 6 \text{ MeV}$, and the depth adjusted to reproduce the binding energy of the last neutron or proton, was used in the present DWBA calculation. Reliability of the information extracted from the DWBA analysis is discussed in detail in Ref. 3. Similar conclusions are obtained in the present analysis. In particular, we have found that use of different distorting potential parameters may in-

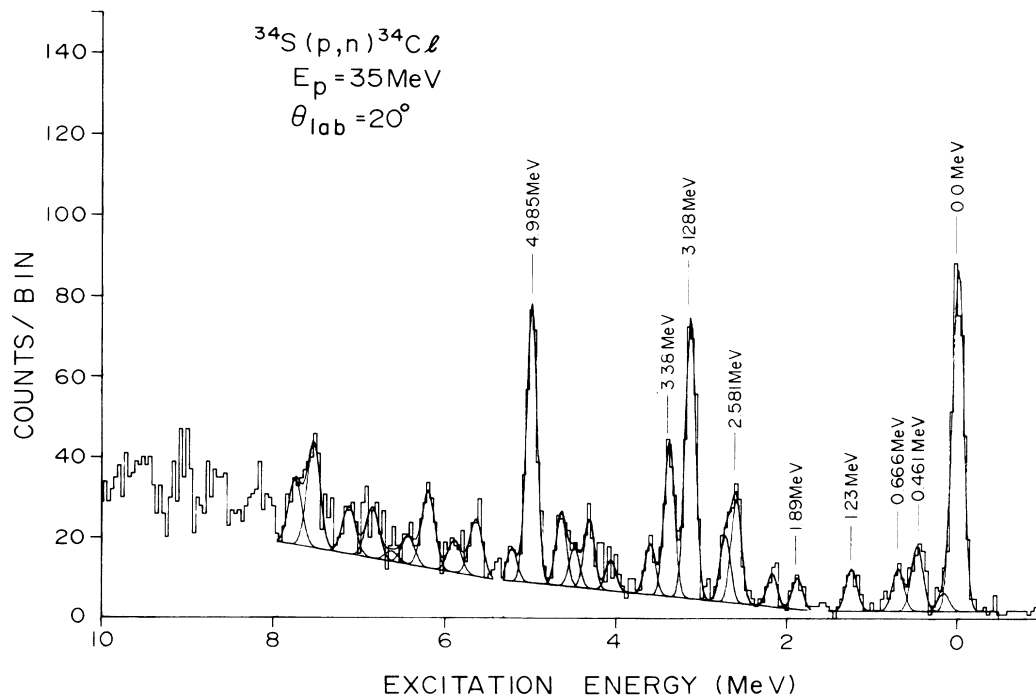


FIG. 1. A sample energy spectrum taken for the $^{34}\text{S}(p,n)^{34}\text{Cl}$ reaction at $E_p = 35$ MeV with a flight path of 44 m. Energy per bin is 25 keV.

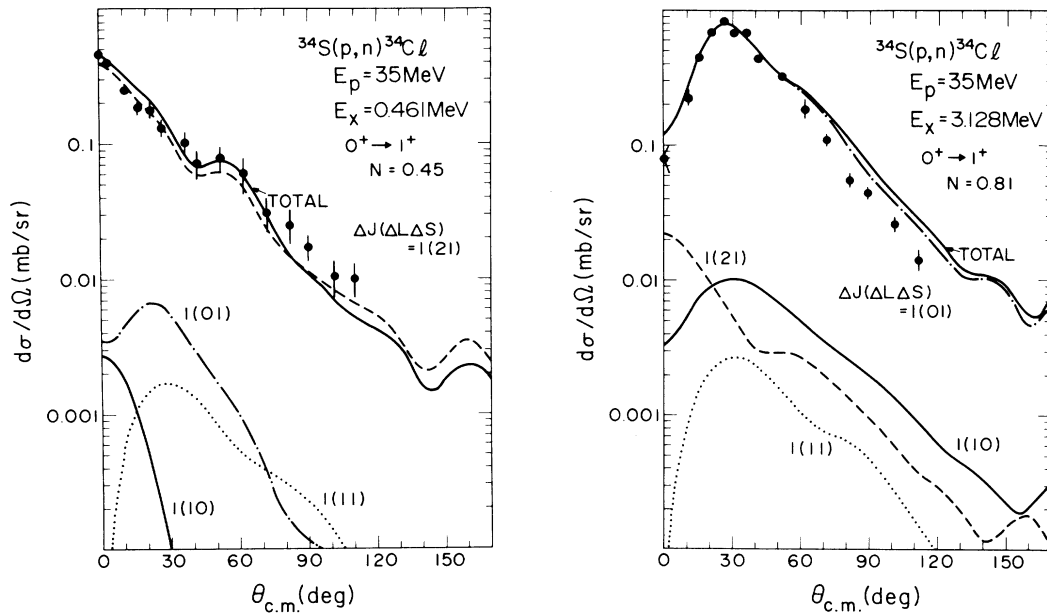


FIG. 2. Differential cross sections for neutrons leading to the 0.461- and 3.128-MeV states through the $0^+ \rightarrow 1^+$ transition. Curves are the DWBA comparison described in the text. Contributions from each $\Delta J(\Delta L \Delta S)$ component are shown separately. "Total" means the coherent sum over these $\Delta J(\Delta L \Delta S)$. N in the figure is a normalization factor introduced to optimize the fitting.

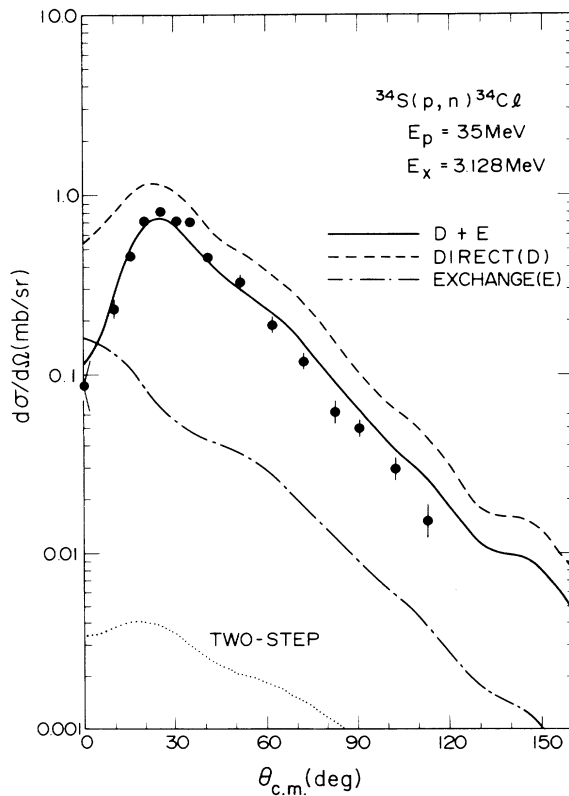


FIG. 3. Comparison of the $0^+ \rightarrow 1^+$ (3.128 MeV) transition with DWBA predictions where direct and exchange contributions are calculated separately. The estimated effect of the two-step process is also shown.

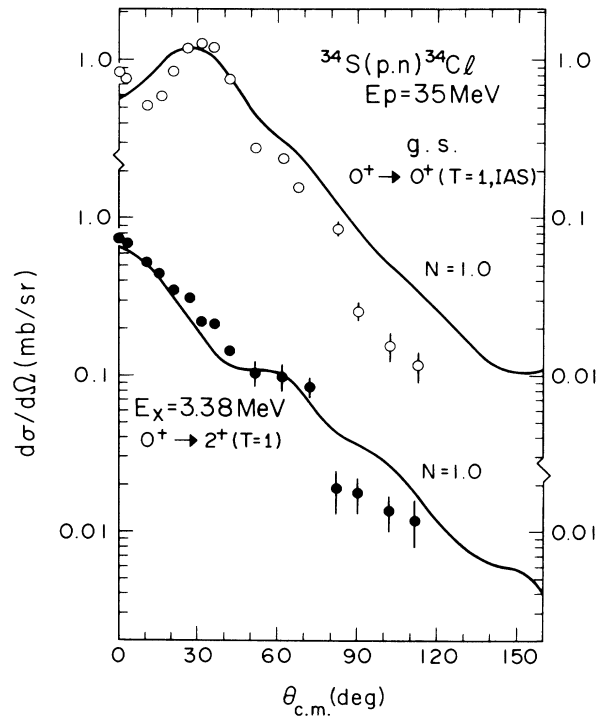


FIG. 4. Experimental and calculated differential cross sections for the $L=0$ and $L=2$ analog transitions.

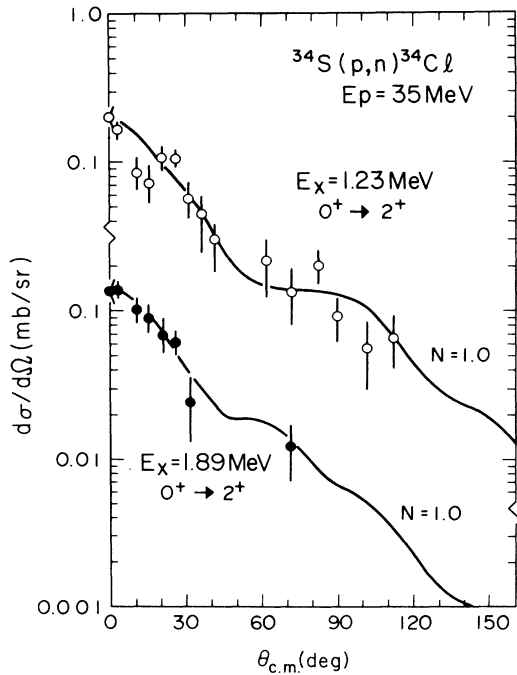


FIG. 5. Same as Fig. 4 but for the transitions leading to the low-lying known 2^+ states in ^{34}Cl .

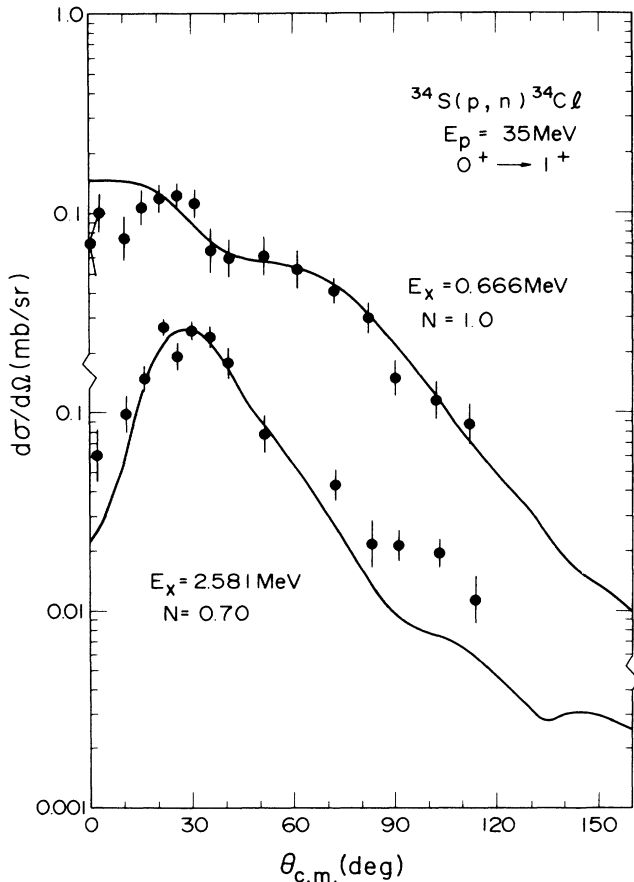


FIG. 6. Differential cross sections for $0^+ \rightarrow 1^+$ transitions other than those shown in Fig. 2 together with DWBA predictions.

produce an ambiguity of $\sim 20\%$ in the absolute magnitude of predicted cross sections as pointed out in Ref. 3. On the other hand, relative errors introduced by a specific choice of the parameter set is rather small. Furthermore, results with other choices of the effective interaction, i.e., the ones given by Anantaraman, Toki, and Bertsch,¹⁰ and by Hosaka, Kubo, and Toki¹¹ show a similar comparison with the present data.

In addition, we have estimated the effects of exchange contributions and that of two-step processes. In Fig. 2 contributions from the $\Delta J(\Delta L, \Delta S) = 1(1,0)$ and $1(1,1)$ components are shown. These unnatural-parity [$\Delta\pi \neq (-)\Delta L$] components contribute to the reaction amplitudes through the exchange terms.¹² It is obvious from Fig. 2 that in general the unnatural-parity components give no sizable contribution to the (p,n) cross section. The total exchange contribution is illustrated in Fig. 3 for the case of the $0^+ \rightarrow 1^+$ transition to the 3.128-MeV state in ^{34}Cl . In this case the dominant part of the cross section comes from the direct term which is proportional to $V_{\sigma T}$, and the interference with the exchange term reduces the final (p,n) cross sections by about 30%.

A sample two-step calculation has been carried out using the code TWFNR (Ref. 13) to obtain a crude esti-

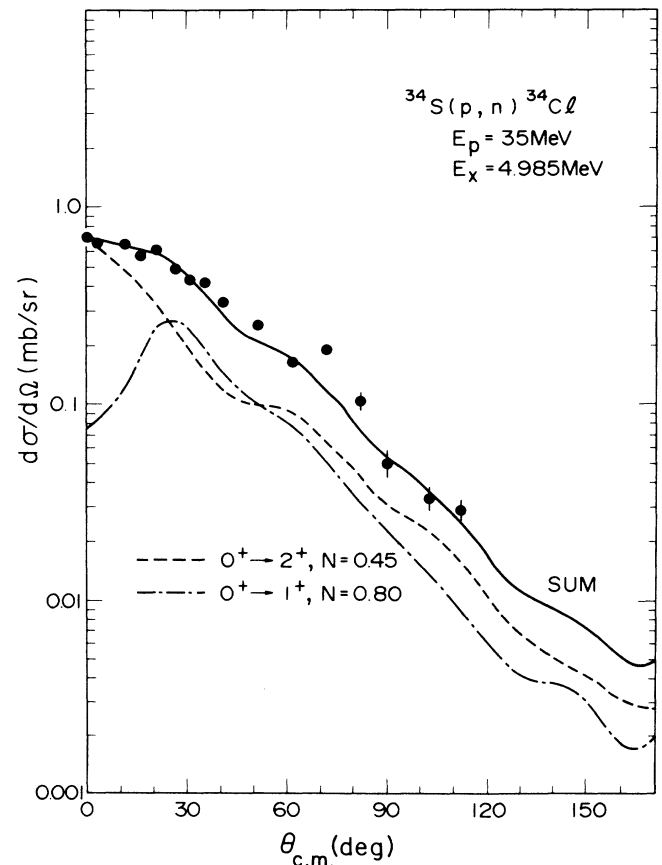


FIG. 7. Differential cross sections for neutrons leading to the $E_x = 4.985$ MeV peak. DWBA comparison is made under the assumption that this peak is a doublet to be decomposed into the $0^+ \rightarrow 1^+$ and $0^+ \rightarrow 2^+$ transitions.

mate of the possible (p,d) (d,n) contribution to the (p,n) cross sections for the 3.128-MeV transition as illustrated in Fig. 3. Both ^{34}S and the deuteron were assumed to be in their ground state in the intermediate channel. The proton and neutron distorting potentials were taken to be the same as for the (p,n) case, and the deuteron potential was taken from Ref. 14. Spectroscopic amplitudes for the (p,d) and (d,n) transitions were calculated using the code OXBASH (Ref. 15) using the BW wave functions. Such a higher-order process brings no sizable contribution to the 35-MeV (p,n) cross section.

IV. DISCUSSION

Figure 4 shows the angular distribution for the $0^+ \rightarrow 0^+$ and $0^+ \rightarrow 2^+$ analog transitions. It should be noted that no scaling of the calculated results has been made to optimize comparison. The fit to the $0^+ \rightarrow 0^+$ analog transition is relatively poor. This may be due to the omission of numerous small components supposedly involved in such strong collective transitions but not included in shell-model calculations with a limited space. A coherent addition of such small components would improve the fit to the data, especially at small angles. Otherwise the present calculations describe the analog transitions very well.

More examples of the $\Delta L = 2$ transitions are nonanalog transitions leading to the low-lying 2^+ states at 1.23 and 1.89 MeV, whose angular distributions and comparisons with calculations are shown in Fig. 5. No scaling is necessary for these states either.

One of the remarkable features of the present results is the observation of the different angular distribution patterns for the $0^+ \rightarrow 1^+$ transitions. This feature is reproduced very well by the calculation. In an attempt to find the origin of these large differences, we decomposed the spectroscopic amplitudes Z_{jj} , given in the jj coupling scheme into the LS representation and calculated cross sections for each $\Delta J(\Delta L, \Delta S)$. Some of the results are illustrated in Fig. 2. Now, the conclusion is straightforward: The $0^+ \rightarrow 1^+$ transition to the 0.461-MeV state is dominated by the $\Delta L = 2$ spin flip component $1(2,1)$, while that to the 3.128-MeV state is dominated by the $\Delta L = 0$ Gamow-Teller-type $1(0,1)$ component. The former exhibits a $\Delta L = 2$ angular distribution shape and the latter $\Delta L = 0$. Indeed the two $0^+ \rightarrow 1^+$ transitions leading to the 0.461- and 3.128-MeV states show angular distribution shapes similar to the pure $\Delta L = 2$ and $\Delta L = 0$ analog transitions, respectively, displayed in Fig. 4. Two other 1^+ angular distributions show intermediate patterns (Fig. 6). But the $1(0,1)$ component is more important in the transition to the 2.581-MeV state, making the angular distribution shape similar to that for the 3.128-MeV state, while the $1(0,1)$ and $1(2,1)$ contributions are roughly the same in the transition to the 0.666-MeV state. The unnatural-parity $\Delta L = 1$ components $1(1,0)$ and $1(1,1)$ contribute to the exchange terms. As discussed before, they are sufficiently small to permit a direct comparison of the (p,n) strength with the corresponding β -decay rate.

Thus the presently applied shell model has explained

quite consistently the four $0^+ \rightarrow 1^+$ transitions. The (p,n) angular distribution shapes for the $0^+ \rightarrow 1^+$ transitions are found to be very sensitive to the transition amplitudes involved. Because of this high sensitivity they provide a stringent test of the shell-model wave functions. N in the figure means the normalization factor introduced to optimize the fitting. It is interesting to note that the observed cross section for the dominant $1(0,1)$ transition to the 3.128-MeV state is about 80% of the calculation, while that for the dominant $1(2,1)$ transition to the 0.461-MeV state is only 45%. This point will be discussed later.

Based on successful comparison of the experimental results and theoretical predictions for transitions leading to the known states in ^{34}Cl , we discuss the strong transition to the 4.985-MeV peak. The measured angular distribution and DWBA comparison are shown in Fig. 7. The present shell-model calculation predicts a rather strong GT transition to a $T=0$, 1^+ state at 4.986 MeV (sixth $T=0$, 1^+ state), although energetically unfavored β decay to this state has not been observed. In addition, a rather strong $0^+ \rightarrow 2^+$ transition leading to a $T=0$, 2^+ state at 5.039 MeV is predicted as well. Indeed the experimental angular distribution is reproduced by the sum of the $0^+ \rightarrow 1^+$ and $0^+ \rightarrow 2^+$ cross sections. Since the cross sections at very small angles come mainly from the $0^+ \rightarrow 2^+$ component, we obtain the normalization factor N at 0° for the $0^+ \rightarrow 2^+$ transition. Then we obtain that for the $0^+ \rightarrow 1^+$ piece by fitting the data at other angles. The normalization N thus obtained are 0.45 and 0.80 for the 2^+ and 1^+ states, respectively. The large reduction factor required for the 2^+ state is in contrast to the other 2^+ states which are fitted without any scaling. Decomposition of the transition amplitudes shows that the $0^+ \rightarrow 2^+$ transition to the 5-MeV state goes mainly through $\Delta J(\Delta L, \Delta S) = 2(2,1)$, while the excitation of the other 2^+ states involves no spin flip. It is interesting to note that the value of N for this $0^+ \rightarrow 2^+$, $2(2,1)$ transition is similar to that for the 0.461-MeV state (1^+) whose main component is $1(2,1)$. We again observe about 20% reduction of the strength for the excitation of the 1^+ state at 4.985 MeV, which is dominated by $\Delta J(\Delta L, \Delta S) = 1(0,1)$. Thus sizable GT strength to the 4.985-MeV state ($\log ft = 3.6$), was found.

It should be noted that no scaling is necessary to optimize comparison for pure $\Delta L = 0$ and 2 transitions with $\Delta S = 0$ (both analog and nonanalog). As mentioned earlier, and pointed out in Ref. 3, although absolute values of calculated cross sections may vary as much as 30% depending on the choice of the parameters involved in DWBA calculations, relative errors introduced are rather small. In this regard it is important that these $\Delta L = 0$ and $\Delta L = 2$ analog and nonanalog transitions are fitted without any scaling, especially the $\Delta L = 2$ transitions which are reproduced through the angular region measured. This strongly suggests that the renormalization factors required for the transitions with $\Delta S = 1$ $1(0,1)$, $1(2,1)$, and $2(2,1)$ are meaningful.

The experimentally observed Gamow-Teller β decay strengths in the sd shell region are quenched on the whole by a factor of about 0.6.¹ Such quenching has

been suspected as being due to three origins:^{16,17} (1) higher-order nucleon configuration mixing; (2) presence of the Δ isobar in the nuclear wave functions; and (3) mesonic exchange currents such as the π - ρ exchange and the pionic pair diagram. The first is thought to be the most important.^{1,16,17} However, among the renormalization factors $B(\text{GT})_{\text{exp}}/B(\text{GT})_{\text{free}}$ for the β -decay strength in sd -shell nuclei, that for the $^{34}\text{Ar}(0^+) \rightarrow ^{34}\text{Cl}$ (3.129 MeV, 1^+) is exceptionally large and almost unity.¹ The ratio $(d\sigma/d\Omega)_{\text{exp}}/(d\sigma/d\Omega)_{\text{DWBA}}$ in the present work is also large compared to those from many other (p,n) experiments so far reported for the GT transitions.^{18,19} This difference in $A=34$ relative to other nuclei in the sd shell may indicate a deficiency in the present $A=34$ wave functions which should be explored if and when new sd -shell interactions are proposed. The present result nevertheless indicates that the transition amplitudes of Brown and Wildenthal describe the (p,n) transitions of the GT type very well on the whole.

V. CONCLUSION

We have studied the $^{34}\text{S}(\text{p},\text{n})^{34}\text{Cl}$ reaction at $E_p=35$ MeV by means of the high-resolution time-of-flight technique. The shell-model wave functions of Brown and Wildenthal give quite a reasonable explanation of the experimental results. Analog transitions leading to the $T=1$, 0^+ and 2^+ states were absolutely fitted by the DWBA calculations with transition amplitudes derived from the shell-model wave functions. Isovector $\Delta S=0$ transitions leading to the low-lying 2^+ states in ^{34}Cl were absolutely fitted as well. The remarkable changes of the $0^+ \rightarrow 1^+$ angular distributions for the states at 0.461, 0.666, 2.581, and 3.128 MeV were satisfactorily reproduced by the DWBA calculations with BW wave

functions. A reasonable renormalization factor consistent with that for the β -decay rate was observed for the 3.128-MeV transition, whose dominant component was $\Delta J(\Delta L, \Delta S)=1(0,1)$. A strong peak was observed at 4.985 MeV. This peak was identified as the $1^+ - 2^+$ doublet predicted by the shell model. According to the BW wave functions the major component of the transition to the 1^+ member of the doublet is $1(0,1)$, and the comparison between the data and the calculation gives the renormalization factor of 0.8, about the same as that for the 3.128-MeV state. Thus a significant fraction of the GT strength was found at $E_x=4.985$ MeV. The 2^+ member of the 4.985-MeV doublet is predicted to have a dominant $2(2,1)$ component. Renormalization factors for the spin-flip $\Delta L=2$ transitions, $1(2,1)$ and $2(2,1)$, are found to be about 0.45, although origin of such a large reduction factor is not clear at present.

We have successfully tested the shell model through low-energy charge-exchange reactions. Further study of sd -shell nuclei may provide data for a number of GT transitions which are energetically inaccessible by β decay.

ACKNOWLEDGMENTS

We thank M. Igarashi for the use of the code TWOFNR. This work was supported in part by the U.S.-Japan Cooperative Science Program of the Japan Society for Promotion of Science and the U.S. National Science Foundation, and by a Grant-in-Aid for Scientific Research, No. 59540147, from the Ministry of Education, Science, and Culture in Japan. One of the authors (B.A.B.) is grateful for support from the Tokyo Institute of Technology Centennial Memorial Fund.

¹B. A. Brown and B. H. Wildenthal, *At. Data and Nucl. Data Tables* **33**, 347 (1985).

²See, for example, G. M. Fuller, W. F. Fowler, and M. J. Newmann, *Astrophys. J. Suppl.* **42**, 447 (1980). This work made use of the Chung-Wildenthal interaction (W. Chung, Ph.D. thesis, Michigan State University, 1976), which was the immediate precursor to the interaction used for Ref. 1.

³H. Ohnuma, M. Kabasawa, K. Furukawa, T. Kawamura, Y. Takahashi, A. Satoh, T. Nakagawa, K. Maeda, K. Miura, T. Niizeki, and H. Orihara, *Nucl. Phys.* **A467**, 61 (1987).

⁴B. A. Brown and B. H. Wildenthal (unpublished).

⁵H. Orihara and T. Murakami, *Nucl. Instrum. Methods* **188**, 15 (1981); H. Orihara, S. Nishihara, K. Furukawa, M. Kabasawa, T. Kawamura, Y. Takahashi, T. Nakagawa, and K. Maeda, *Nucl. Instrum. Methods A* **257**, 189 (1987).

⁶R. Saeffer and J. Raynal, Centre d'Etudes Nucléaires de Saclay Report CEA-R4000, 1970.

⁷F. D. Becchetti, Jr. and G. W. Greenlees, *Phys. Rev.* **192**, 1190 (1969).

⁸J. D. Carlson, C. D. Zafiratos, and D. A. Lind, *Nucl. Phys.* **A249**, 29 (1975).

⁹G. Bertsch, J. Borysowicz, H. McManus, and W. G. Love,

Nucl. Phys. **A284**, 399 (1977).

¹⁰N. Anantaraman, H. Toki, and G. Bertsch, *Nucl. Phys.* **A398**, 269 (1983).

¹¹A. Hosaka, K-I. Kubo, and H. Toki, *Nucl. Phys.* **A444**, 76 (1985).

¹²G. R. Satchler, *Nucl. Phys.* **85**, 273 (1966).

¹³M. Igarashi, computer code TWOFNR (unpublished).

¹⁴W. W. Daehnick, J. D. Childs, and Z. Vrcelj, *Phys. Rev. C* **21**, 2253 (1980).

¹⁵The shell-model code OXBASH, A. E. Etchegoyen, W. A. M. Rae, N. S. Goduin, W. A. Richter, C. H. Zimmerman, B. A. Brown, W. E. Ormand, and J. S. Winfield, National Superconducting Cyclotron Laboratory Report 524, 1984.

¹⁶I. S. Towner and F. C. Khanna, *Nucl. Phys.* **A399**, 334 (1983).

¹⁷A. Arima *et al.*, *Adv. Nucl. Phys.* (to be published).

¹⁸C. D. Goodman and S. D. Bloom, in *Conference on Spin Excitation in Nuclei*, edited by F. Petrovichi *et al.* (Plenum, New York, 1984), p. 143.

¹⁹H. Orihara, T. Murakami, S. Nishihara, T. Nakagawa, K. Maeda, K. Miura, and H. Ohnuma, *Phys. Rev. Lett.* **47**, 301 (1981).